The International Journal of Advanced Manufacturing Technology (2018) 97:3119–3128
https://doi.org/10.1007/s00170-018-2187-3

ORIGINAL ARTICLE

Study on micro helical milling of small holes with flat end mills

Xiang Cheng[1] · Xi Zhang[2] · Yebing Tian[1] · Guangming Zheng[1] · Xianhai Yang[1]

Received: 29 November 2017 / Accepted: 13 May 2018 / Published online: 23 May 2018

Abstract
Helical milling as an eco-friendly hole-making process has various advantages comparing to conventional drilling process and has been widely studied. But micro helical milling for small holes was not investigated. This paper focuses on preliminary studies on micro helical milling of small holes with flat micro end mills. The cutting phenomena of the radial and axial cutting edges are considered and discussed separately. Based on the size effect existing in microcutting processes, the minimum undeformed chip thicknesses (h_{min}) for both radial and axial cutting edges are identified for work material copper C26000 by finite element method and micro helical milling experiments. Since burrs are noticed during experimental studies, burrs at the hole entrance are analyzed elementarily and it shows that the burr size has a relation with the critical conditions in micro helical milling. The study turns out that the ratio of h_{min} to cutting edge radius in micro helical milling is from 0.6 to 0.68 and is larger than that of conventional microcutting processes for various materials, which is usually in the range from 0.14 to 0.43. It is a good sign for micro helical milling of small holes with higher productivities since the ratio of h_{min} to tool cutting edge radius is larger than that of conventional microcutting processes.

Keywords Micro helical milling · Size effect · Minimum undeformed chip thickness · Finite element method · Cutting edge

1 Introduction

Helical milling is an eco-friendly hole-making machining process with advantages such as flexible kinematics, low cutting forces, low tool wear, and improved hole finish quality compared to conventional drilling [1]. Due to these advantages, helical milling has been studied widely from kinematics [2], cutting forces [3], temperature [4], wear and tool life [5], modeling [6], etc. However, macro helical milling was mainly studied with hole diameters from 4.77 to 35 mm [7–10]. Micro helical milling was not investigated and there are a lot of requirements which may be studies [11].

From the size of micro end mills used, micromilling refers to milling by micro end mills with the cutting diameter smaller than 1 mm [12]. Micro helical milling is within this definition. Size effect and the minimum undeformed chip thickness (MUCT) are well-known existing in microcutting processes. Bissaco et al. have conducted micromilling studies for microinjection molding molds in hardened steel. They experimentally showed material was subjected to an elastic-plastic deformation without chips formation when the cutting thickness was less than the MUCT due to the size effect [13]. This topic has been studied widely.

For micromilling, it includes four key parameters as the cutting speed V_C, feed per tooth f_Z, radial depth of cut a_e, and axial depth of cut a_p. Cheng et al. have created micromilling models and evaluated by experimental data [14]. It shows that radial cutting edge and axial cutting edge work together to conduct microcutting in micromilling. Therefore, the MUCTs for both radial cutting edge and axial cutting edge in micro helical milling are studied by conducting finite element method (FEM) simulations and experiments in this paper. First, the parameters and UCT associated with micro helical milling are discussed. Second, the MUCT is identified for both radial and axial cutting edges by FEM modeling analyses taking chip generations and cutting force variations as the judgment criteria, respectively. Third, micro helical milling experiments have been conducted for the evaluation of FEM analyses. Burr width at the hole entrance has also

✉ Xiang Cheng
chengxiang@sdut.edu.cn

[1] School of Mechanical Engineering, Shandong University of Technology, Zibo 255000, China

[2] School of Mechatronics and Mechanical Engineering, Shanghai University, Shanghai 200444, China

been measured and analyzed. Finally, both simulation and experimental results are discussed.

2 Modeling and analyses

2.1 Parameters associated

In micro helical milling process, micro end mill proceeds a helical path while rotates around its own axis. There are three ratios of tool diameters to hole radii in helical milling, namely, < 1, = 1, and > 1. Since stiffness is relatively low for micro end mills, the last ratio is applied in this study. The following parameters are included in micro helical milling: hole diameter D_h, cutter diameter D_t, cutter orbits diameter D_r, number of cutter teeth z, spindle speed n_1, cutter orbits speed n_2, cutting tangential feed speed V_{fc}, tangential feed per tooth f_{zc}, cutting axial feed speed V_{fa}, axial feed per tooth f_{za}, radial depth of cut a_e, axial depth of cut a_p, and the maximum axial depth of cut in steady micro helical milling state a_{pmax}. The relationships among them are as follows.

$$D_r = D_h - D_t \tag{1}$$

$$n_2 = \frac{f_{zc} \times z \times n_1}{\pi \times D_r} \tag{2}$$

$$V_{fc} = f_{zc} \times z \times n_1 \tag{3}$$

$$V_{fa} = f_{za} \times z \times n_1 \tag{4}$$

$$a_{pmax} = \frac{f_{za} \times \pi \times D_r}{f_{zc}} \tag{5}$$

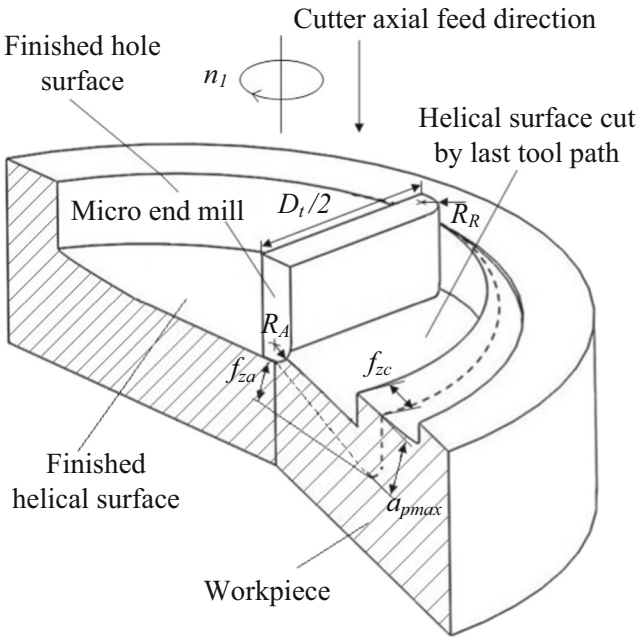

Fig. 1 Undeformed chip formations in micro helical milling at steady state

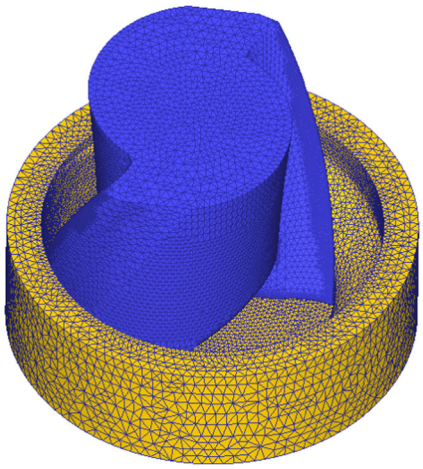

Fig. 2 FEM modeling for micro helical milling

2.2 Modeling

Kinematic motions of micro helical milling are the same as macro ones. But the study viewpoints are quite different. For macro ones, cutting edges are considered as fully sharp. Cutter geometrical features such like rake angles and clearance angles are always taken into consideration. However, for micro ones, cutting edges radii must be taken into consideration regardless of rake and clearance angles since the sizes of both the radial and axial depths of cut are commensurate with those of the cutting edges radii. Therefore, cutting edge radii are the key cutter geometrical features to be studied. Consequently, the undeformed chip thicknesses dominate the micro helical milling process as that in micromilling applications. Undeformed chip formation is always changing from the beginning to the steady micro helical milling state. Then, the undeformed chip formation remains unchanged. Hereafter, the minimum undeformed chip thickness refers to the critical UCT when micro helical milling is in the steady state. Figure 1 shows the undeformed chips at the steady state.

From Fig. 1, the UCT of radial and axial cutting edge is the value of tangential feed f_{zc} and axial feed f_{za}, respectively.

Workpiece is pre-processed to shorten the simulation time and to make sure the micro helical milling is at the steady state. The FEA software Deform 3D has been used for the

Table 1 FEM analyses parameters for radial cutting edge

No.	f_{za} (μm/z)	f_{zc} (μm/z)	a_{pmax} (μm)
1	4	2.8	449
2	4	3.0	419
3	4	3.2	393
4	4	3.4	370
5	4	3.6	349
6	4	3.8	331

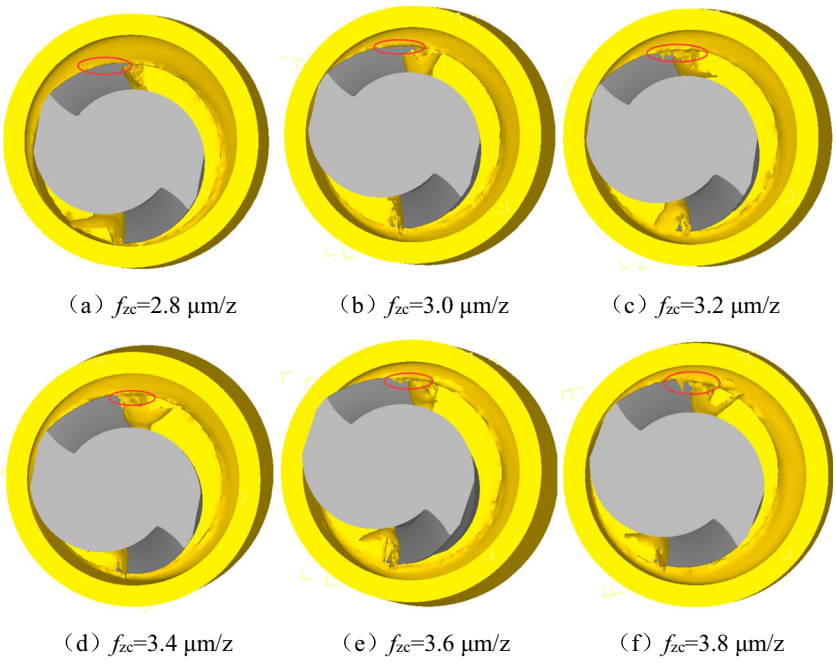

Fig. 3 Chips generation by radial cutting edge. **a** $f_{zc} = 2.8$ μm/z. **b** $f_{zc} = 3.0$ μm/z. **c** $f_{zc} = 3.2$ μm/z. **d** $f_{zc} = 3.4$ μm/z. **e** $f_{zc} = 3.6$ μm/z. **f** $f_{zc} = 3.8$ μm/z

FE modeling. Material properties of the workpiece and the end mill are selected from the material library of the software. The model uses tetrahedron elements with a pre-defined side length of 1 μm at the cutting zone. The adaptive meshing method has been applied and the mesh can be refined according to the real-time calculating demands. The classical Johnson-Cook constitutive material model is applied. The meshed tool-workpiece assembly in the software Deform 3D is shown in Fig. 2.

Since radial and axial cutting edges are under different cutting conditions in micromilling processes as mentioned in [14], the MUCT analyses are conducted independently for radial and axial cutting edges.

Due to the size effect in microcutting [13], chips will be created along the engaged cutting edge and the cutting force will be the smallest when MUCT is reached. Therefore, in the FEM analyses, chips and cutting forces are selected as the judgment criteria for MUCT separately.

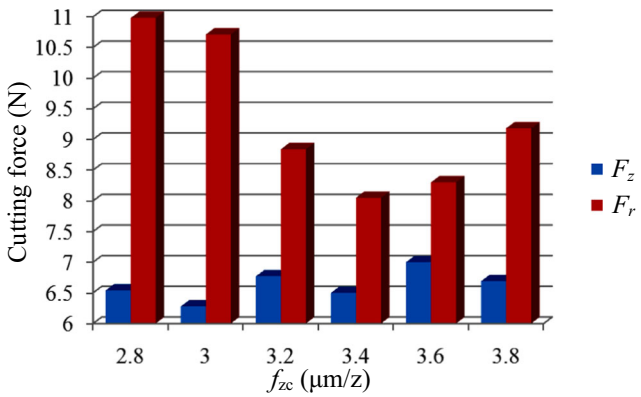

Fig. 4 Micro helical milling forces vs. f_{zc}

2.3 FEM analyses for radial cutting edge

In FEM analyses and experiments for micro helical milling, $D_h = 0.7$ mm, $D_t = 0.6$ mm, $z = 2$, $D_r = 0.1$ mm, $n_1 = 80{,}000$ min^{-1}, $a_e = D_t = 0.6$ mm, and radii of radial and axial cutting edges $R_A = R_R = 5$ μm. Work material is copper C26000.

In the simulation, axial feed f_{za} is fixed and tangential feed f_{zc} varies as shown in Table 1. Based on previous studies, f_{za} is fixed at 4 μm/z, which is large enough to make sure the axial cutting edge can generate chips with the edge radius of 5 μm. The unit "μm/z" is the feed per tooth per revolution.

Figure 3 shows the simulated chip generation process.

From Fig. 3, chips are not created when f_{zc} is equal to and smaller than 3.0 μm/z. Chips are created by radial cutting edge when f_{zc} is equal to and larger than 3.2 μm/z. Therefore, the MUCT is 3.2 μm for radial cutting edge according to the size effect theory in microcutting.

Axial cutting force F_z and radial cutting forces F_x and F_y in micro helical milling are to be analyzed. At the steady state of

Table 2 FEM analyses parameters for radial cutting edge

No.	f_{zc} (μm/z)	f_{za} (μm/z)	a_{pmax} (μm)
1	4	2.6	204
2	4	2.8	220
3	4	3.0	236
4	4	3.2	251
5	4	3.4	267
6	4	3.6	283

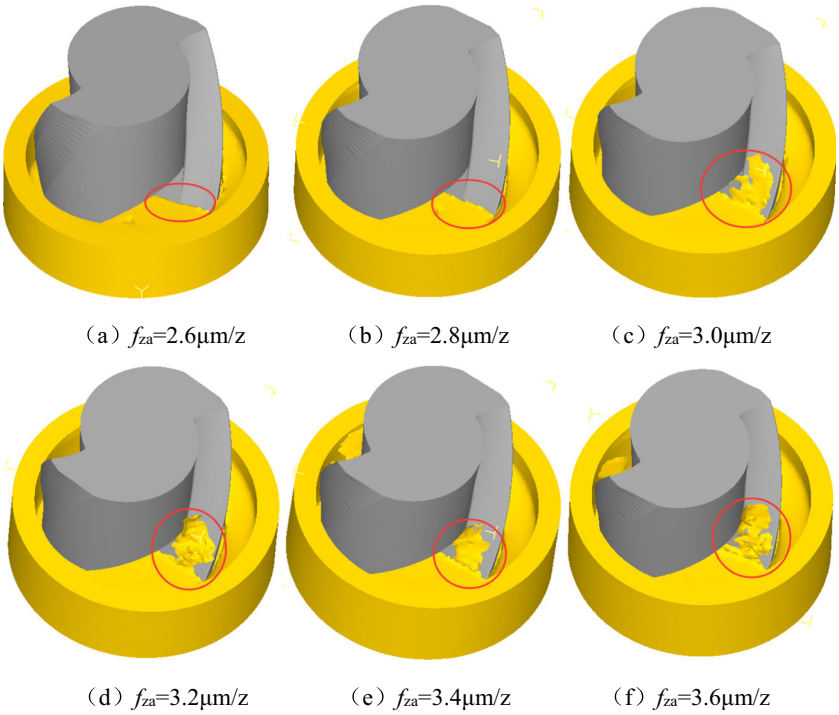

Fig. 5 Chips generation by axial cutting edge. **a** $f_{za} = 2.6$ μm/z. **b** $f_{za} = 2.8$ μm/z. **c** $f_{za} = 3.0$ μm/z. **d** $f_{za} = 3.2$ μm/z. **e** $f_{za} = 3.4$ μm/z. **f** $f_{za} = 3.6$ μm/z

micro helical milling, these three forces are recorded. F_z is relatively stable since continuous cutting is conducted by axial cutting edges with constant axial feed f_{za}. But radial cutting edge always cuts in and out; F_x and F_y vary with the variation of f_{zc}. Therefore, their maximum values are recorded and resultant radial force F_r is calculated by

$$F_r = \sqrt{{F_{xmax}}^2 + {F_{ymax}}^2} \tag{6}$$

The simulated cutting forces are shown in Fig. 4.

From Fig. 4, axial cutting force F_z is slightly fluctuated since the microcutting by axial cutting edge is stable. The slight fluctuation is mainly caused by the friction between side cutting edge and the workpiece in axial direction. Radial cutting force F_r becomes small first and large then before and after $f_{zc} = 3.4$ μm/z with the increasement of f_{zc}. The reason has been explained as the well-known size effect in microcutting. It is mainly caused by the tool-workpiece engagement situations of radial cutting edges. Based on the cutting force analyses, it can be concluded that the MUCT for radial cutting edge is approximately 3.4 μm, which is almost in accordance with that identified from chip generation analyses.

2.4 FEM analyses for axial cutting edges

In the simulation, tangential feed f_{zc} is fixed and axial feed f_{za} varies as shown in Table 2. Based on the above

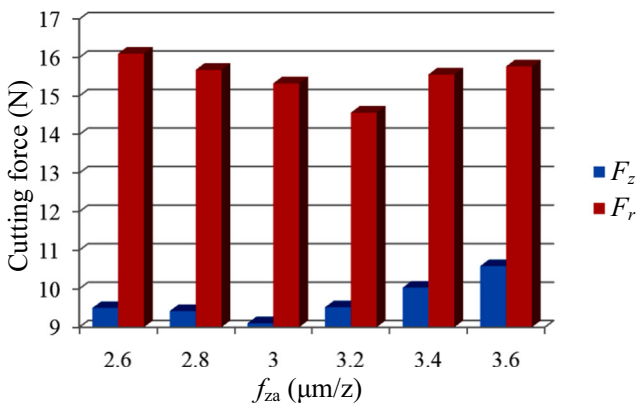

Fig. 6 Micro helical milling forces vs. f_{za}

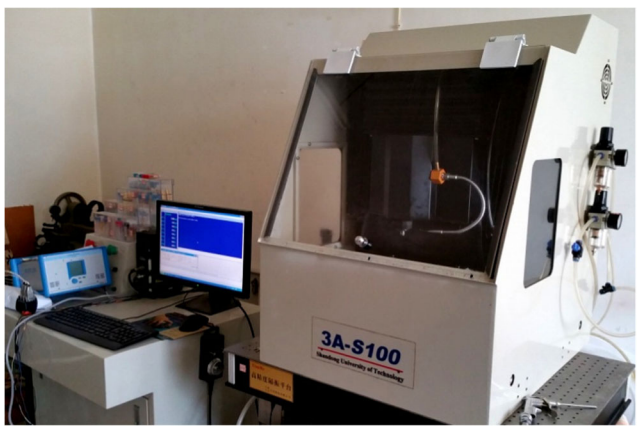

Fig. 7 Micromilling machine tool 3A-S100

studies, f_{zc} is fixed at 4 μm/z, which is large enough to make sure the radial cutting edge can generate chips with the edge radius of 5 μm.

Figure 5 shows the simulated chips generated in process.

From Fig. 5, chips are not created when f_{za} is equal to and smaller than 2.8 μm/z. Chips are created by axial cutting edge when f_{za} is equal to and larger than 3.0 μm/z. Therefore, the MUCT is 3.0 μm for axial cutting edge according to the size effect theory in microcutting.

The simulated cutting forces are shown in Fig. 6.

From Fig. 6, axial cutting force F_z becomes small first and large then before and after $f_{za} = 3.0$ μm/z with the increasement of f_{za}. The reason has been explained as the well-known size effect in microcutting. It is mainly caused by the tool-workpiece engagement situations of axial cutting edges. Based on the cutting force

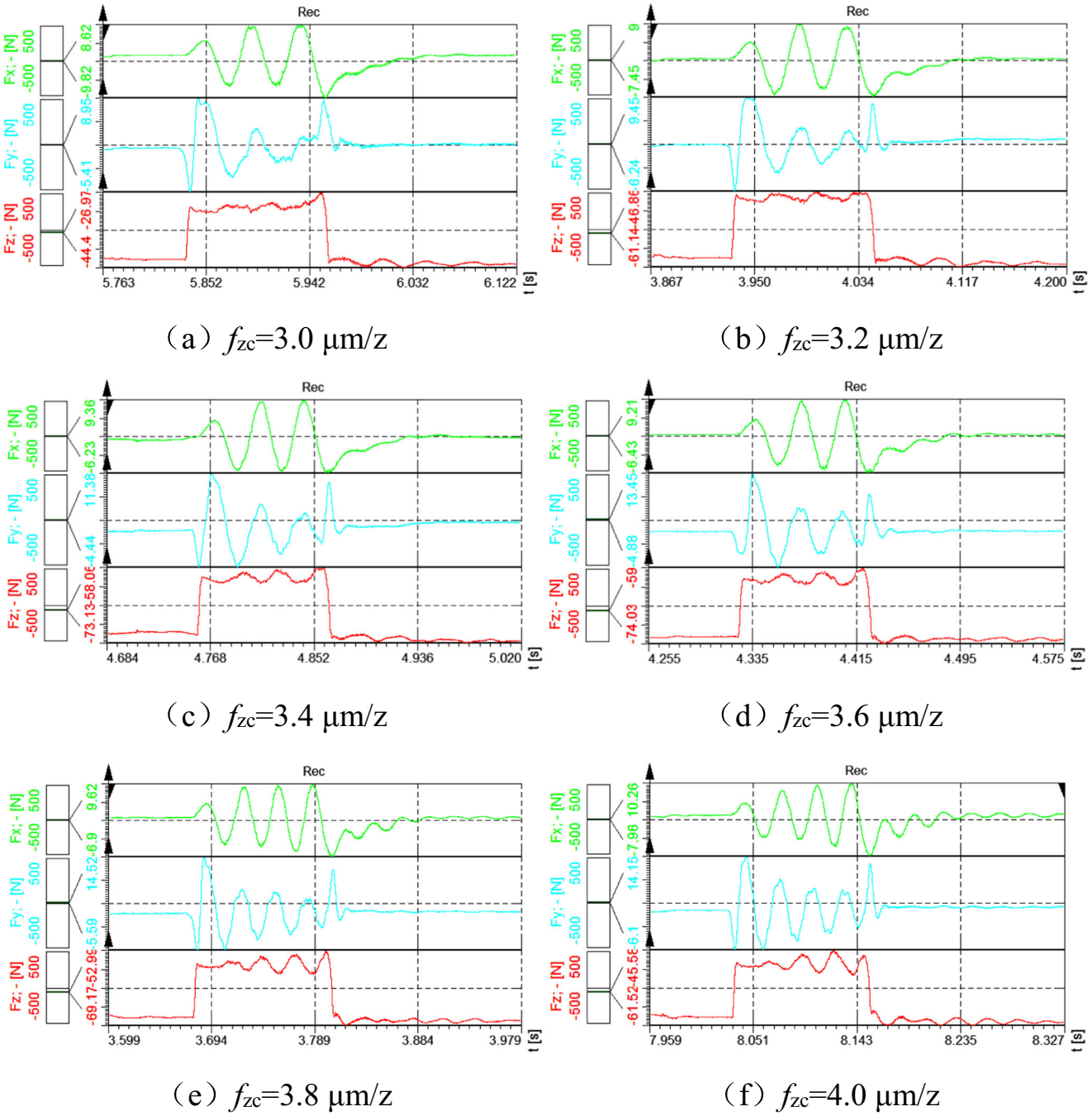

（a）f_{zc}=3.0 μm/z （b）f_{zc}=3.2 μm/z

（c）f_{zc}=3.4 μm/z （d）f_{zc}=3.6 μm/z

（e）f_{zc}=3.8 μm/z （f）f_{zc}=4.0 μm/z

Fig. 8 Microcutting forces recorded by radial cutting edge. **a** $f_{zc} = 3.0$ μm/z. **b** $f_{zc} = 3.2$ μm/z. **c** $f_{zc} = 3.4$ μm/z. **d** $f_{zc} = 3.6$ μm/z. **e** $f_{zc} = 3.8$ μm/z. **f** $f_{zc} = 4.0$ μm/z

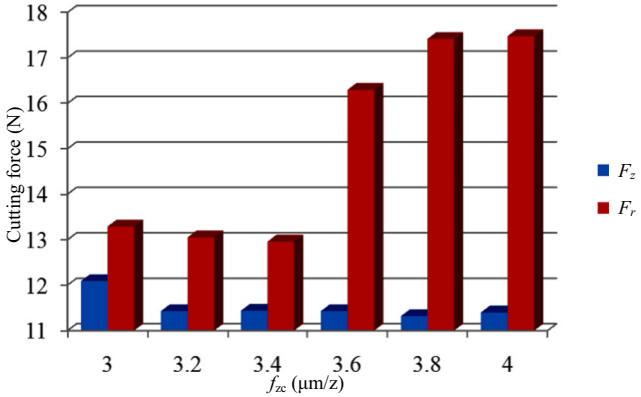

Fig. 9 Average microcutting forces by radial cutting edge

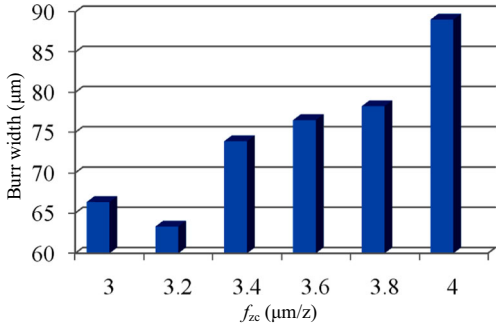

Fig. 11 Burr width measurements

analyses, it can be concluded that the MUCT for axial cutting edge is approximately 3.0 μm, which is in good accordance with that identified from chip generation analyses. Since radial cutting force F_r is a coupling effect of both radial and axial cutting edges, the variation of F_r is irregular with the increasement of f_{za}.

3 Experiments

3.1 Experimental setup

A desktop three-axis micromilling machine tool 3A-S100 shown in Fig. 7 is used for the experiments [15]. Each axis is driven by a linear motor and has the final positioning accuracy of 0.6 μm. The 3A-S100 uses an air-driven and air-

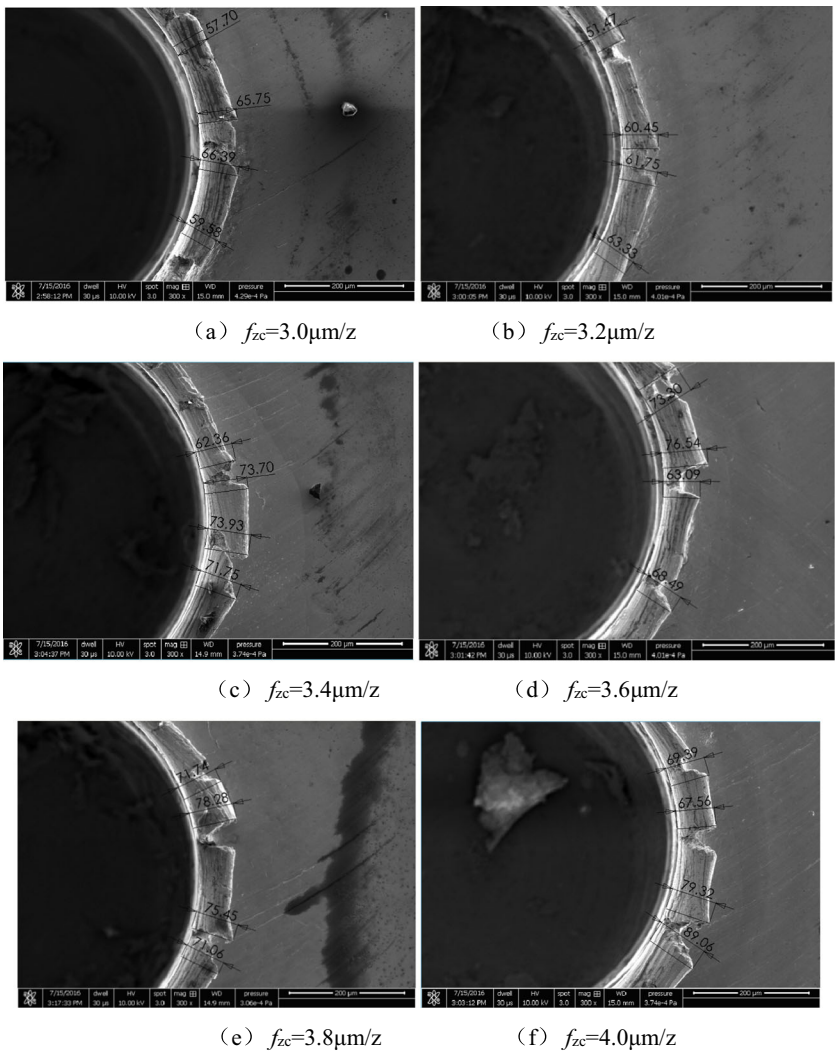

Fig. 10 Burrs measurements by SEM. **a** f_{zc} = 3.0 μm/z. **b** f_{zc} = 3.2 μm/z. **c** f_{zc} = 3.4 μm/z. **d** f_{zc} = 3.6 μm/z. **e** f_{zc} = 3.8 μm/z. **f** f_{zc} = 4.0 μm/z

bearing spindle, whose maximum speed is 80,000 min^{-1}. Radial and axial runout of the spindle is smaller than 1 μm. The dynamometer Kistler 9257B is used for cutting force measurements. Work material is copper C26000. Tool material is tungsten carbide. The micro end mill has the cutting edge radius of 5 μm and cutting diameter of 0.6 mm. Since the cutting diameter is small, in order to reach a reasonable cutting speed, spindle speed is fixed at 80,000 min^{-1}. The depth of the machined small hole is 1 mm in the experiments.

3.2 Micro helical milling by radial cutting edges

Micro helical milling parameters for experiments by radial cutting edges are that the axial feed f_{za} is fixed at 4 μm/z and the tangential feed f_{zc} varies from 3.0 to 4.0 μm/z with the increment of 0.2 μm/z. Microcutting forces are collected as shown in Fig. 8. Microcutting forces are averaged from the collected data of three experiments and summarized in Fig. 9.

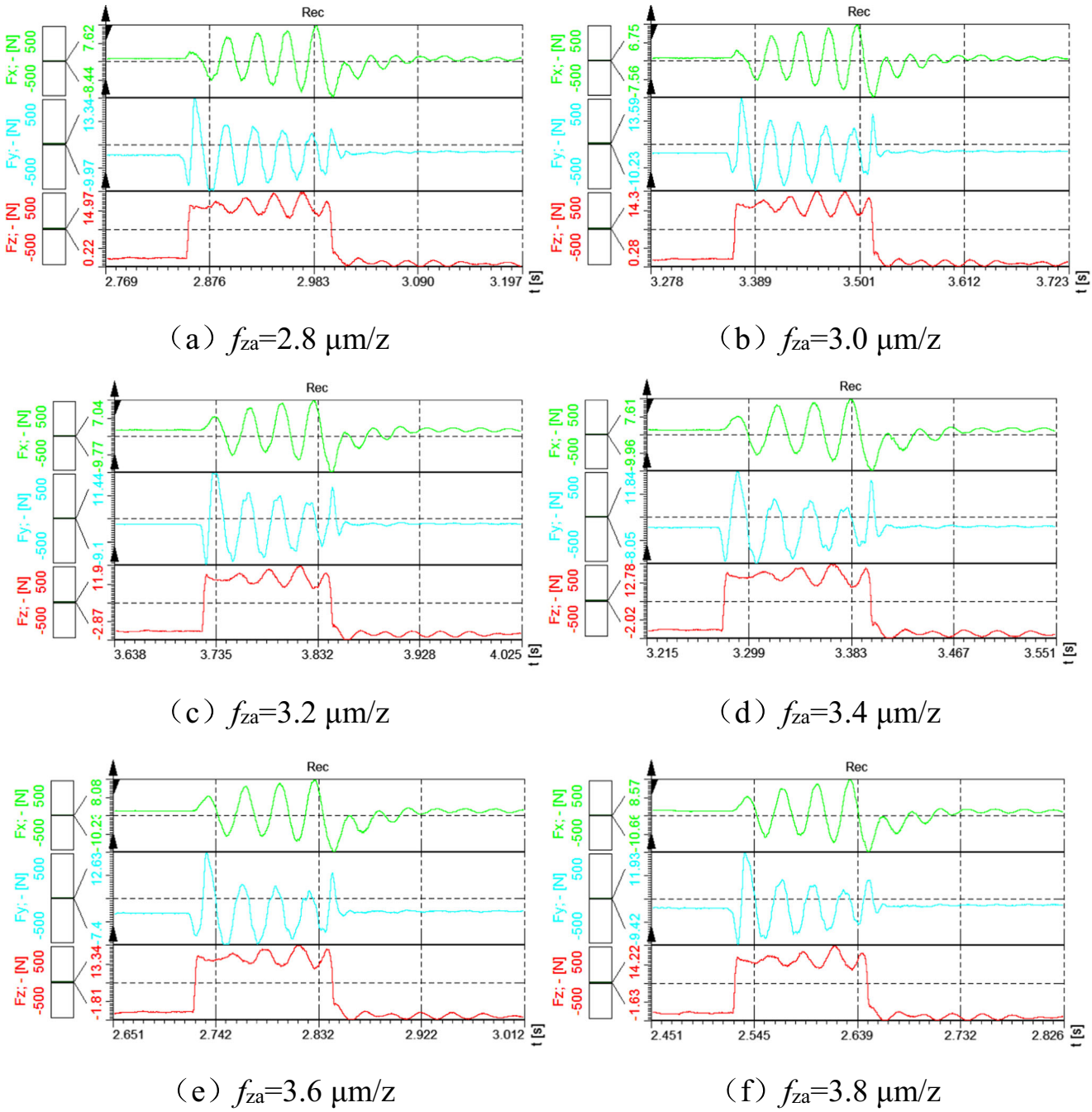

Fig. 12 Microcutting forces recorded by axial cutting edge. **a** f_{za} = 2.8 μm/z. **b** f_{za} = 3.0 μm/z. **c** f_{za} = 3.2 μm/z. **d** f_{za} = 3.4 μm/z. **e** f_{za} = 3.6 μm/z. **f** f_{za} = 3.8 μm/z

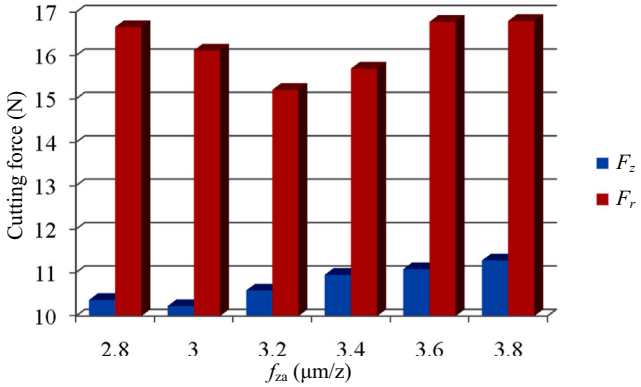

Fig. 13 Average microcutting forces by axial cutting edge

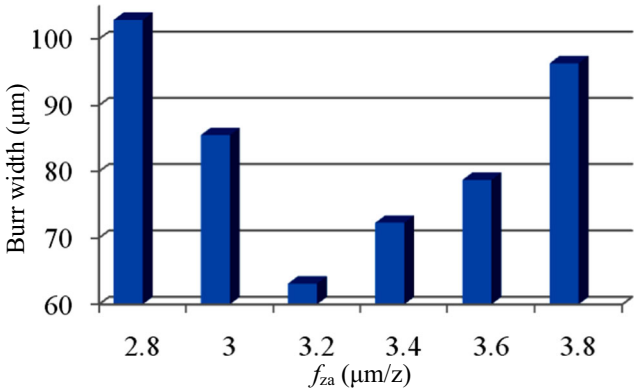

Fig. 15 Burr width measurements

From Fig. 9, axial cutting force F_z has a slight fluctuation since the microcutting by axial cutting edge is stable when f_{za} is fixed. Radial cutting force F_r is larger than axial cutting force F_z. There exists an inflection point of F_r when f_{zc} is 3.4 μm/z. The MUCT is 3.4 μm for radial cutting edge, which is in accordance with that identified by simulations. The difference is that the force values from experiments are larger than those of simulations. One of the possible reasons is that the radial stiffness of the micro end mill is small and tool chatter introduces extra forces into the experimental measurements.

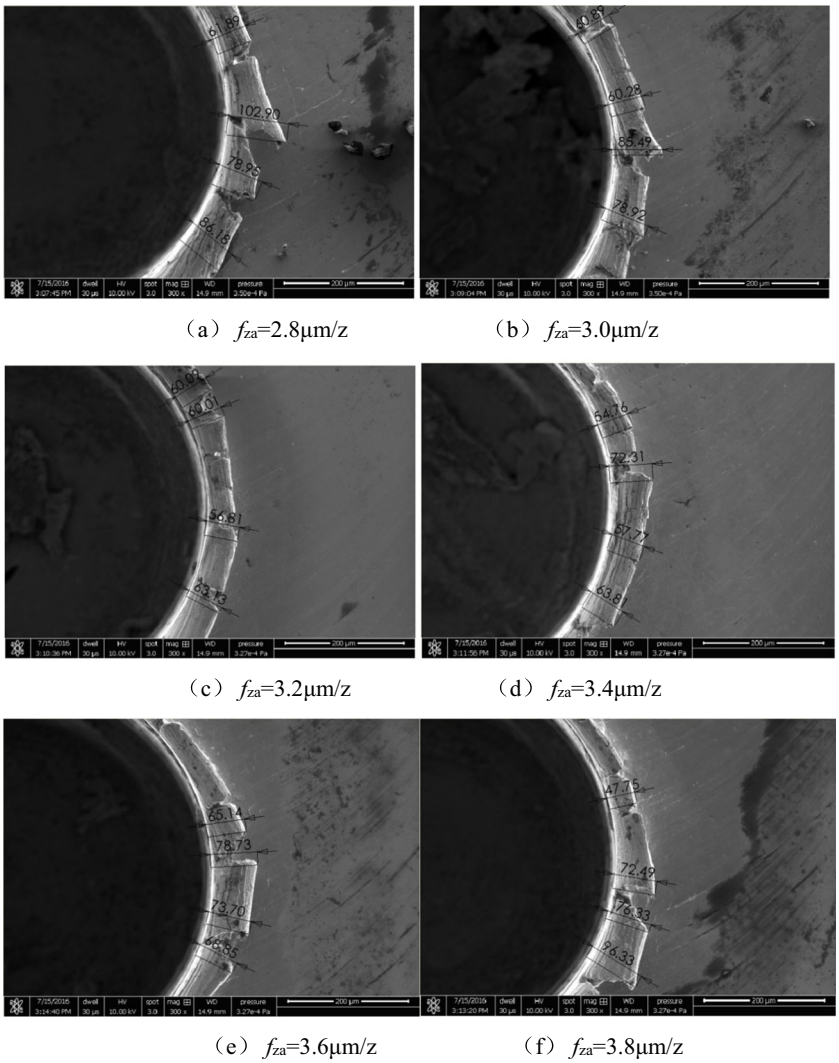

（a） f_{za}=2.8μm/z （b） f_{za}=3.0μm/z

（c） f_{za}=3.2μm/z （d） f_{za}=3.4μm/z

（e） f_{za}=3.6μm/z （f） f_{za}=3.8μm/z

Fig. 14 Burrs measurements by SEM. **a** f_{za} = 2.8 μm/z. **b** f_{za} = 3.0 μm/z. **c** f_{za} = 3.2 μm/z. **d** f_{za} = 3.4 μm/z. **e** f_{za} = 3.6 μm/z. **f** f_{za} = 3.8 μm/z

Table 3 Summarization of the identified MUCT

Analytical method	Analytical item	Cutting edge	Ratio of MUCT to edge radius
FEM simulation	Chip	Radial	0.64
		Axial	0.60
	Force	Radial	0.68
		Axial	0.64
Micro helical milling experiment	Force	Radial	0.68
		Axial	0.64

Furthermore, burrs are analyzed as shown in Fig. 10 based on scanning electron microscope (SEM) measurements, where only the larger burr width portions are shown. Figure 11 shows the variation tendency of the maximum width of burrs of each experiment with the tangential feed f_{zc}.

From Figs. 10 and 11, burr width varies from 63.3 to 89.1 μm. It becomes small first and large then with the increasement of f_{zc}. The interesting point is that burr width reaches the minimum value when $f_{zc} = 3.2$ μm/z, which is the same inflection point as that in chip generation analyses for radial cutting edge.

3.3 Micro helical milling by axial cutting edges

Micro helical milling parameters for experiments by axial cutting edges are that the tangential feed f_{zc} is fixed at 4 μm/z and the axial feed f_{za} varies from 2.8 to 3.8 μm/z with the increment of 0.2 μm/z. Microcutting forces are collected as shown in Fig. 12 and averaged from the collected data of three experiments and summarized in Fig. 13.

From Fig. 13, both radial cutting force F_r and axial cutting force F_z become small first and large then with the increasement of f_{za}. The inflection point for F_z and F_r is 3.0 and 3.2 μm/z, respectively. The MUCT is 3.0 μm for axial cutting edge, which is in accordance with that identified by simulations.

Furthermore, burrs are analyzed as shown in Fig. 14 based on scanning electron microscope (SEM) measurements. Figure 15 shows the variation tendency of the maximum width of burrs of each experiment with the axial feed f_{za}.

From Figs. 14 and 15, burr width varies from 63.1 to 102.9 μm. It becomes small first and large then with the increasement of axial feed f_{za}. There also exists an inflection point when $f_{za} = 3.2$ μm/z, which is slightly larger than that at the inflection point in chip generation analyses for axial cutting edge.

3.4 Discussions

From the above analyses by FEM simulations and experiments, the identified MUCT is summarized in Table 3.

From Table 3, the MUCTs identified by FEM simulations and experiments show a good agreement. It testifies that FEM simulation can be solely applied to micro helical milling for identifying the MUCT. The MUCT for radial cutting edge is larger than that for axial cutting edge in micro helical milling by micro flat end mills. The ratio of MUCT to tool cutting edge radius (5 μm) is from 0.6 to 0.68 for micro helical milling of small holes on copper C26000. By conventional microcutting processes for various materials, the ratio of MUCT to tool cutting edge radius is in the range from 0.14 to 0.43 as summarized in Table 4 from literature [16].

From Tables 3 and 4, the MUCT for micro helical milling is larger than that for conventional microcutting. It is a good sign for micro helical milling of small holes since the ratio of MUCT to tool cutting edge radius is larger and it is possibly promising for higher productivities.

Burrs at the hole entrance are analyzed by single-factor experiments for radial and axial cutting edges. Both experiments by the variation of tangential feed f_{zc} and axial feed f_{za}

Table 4 The MUCT for microcutting [16]

Author	Year	Method	Work material	Ratio of MUCT to edge radius
Oliveira	2015	Micromilling	AISI 1045 steel	0.22–0.36
Vogler et al.	2004	FEM	Ferrite-pearlite steel	0.14–0.43
Liu et al.	2006	Molecular-mechanical	AISI 1040 steel	0.20–0.35
Liu et al.	2006	Molecular-mechanical	6082-T6 aluminum	0.35–0.40
Malekian et al.	2012	Modeling	6061 aluminum	0.23
Ramos et al.	2012	Orthogonal turning	AISI 1045 steel	0.29
Lai et al.	2008	FEM	OFHC copper	0.25
Kang et al.	2011	Micromilling	AISI 1045 steel	0.30
Woon et al.	2008	FEM	AISI 4340 steel	0.26
Son et al.	2005	Modeling	Aluminum, OFHC copper, brass	0.20–0.40
Kim et al.	2004	Micromilling	360 Brass	0.30
Yuan et al.	1996	Turning	Cu-Mg-Mn aluminum alloy	0.25–0.33

show that there exists an inflection point of the burr width variations. The UCT at the inflection point is just the critical one (MUCT). It preliminarily shows a contradiction between microcutting efficiency and burr size since the optimized micro helical milling parameters will be definitely larger than the critical ones in actual cutting applications for higher machining efficiency. Further studies are needed for this topic.

4 Conclusions

Considering the size effect of microcutting processes, micro helical milling is preliminarily studied by FEM simulations and experiments. From the microscopic view of micro helical milling, the cutting phenomena of the radial and axial cutting edges are considered and discussed separately. Both quantized and qualitative analyses show a good agreement. The MUCT of radial cutting edge is slightly larger than that of axial cutting edge. There exists a distinct difference in microscopic view between micro helical milling and conventional micromilling. The MUCT in micro helical milling is 0.6 to 0.68 of cutting edge radius, which is larger than that, namely 0.14 to 0.43, in conventional microcutting. Burrs at the hole entrance are also analyzed elementarily. The minimum burr size at the hole entrance is approximately 63 μm while the MUCT is reached. Otherwise, burr size becomes larger with the decrease or increasement of single-factor f_{zc} or f_{za} at two sides of its critical value. In conclusion, microcutting efficiency of micro helical milling is theoretically larger than that of conventional microcutting processes. This study suggests both radial and axial cutting edges should be investigated separately in micro helical milling processes. Further studies are needed to minimize the burr sizes and to achieve optimized micro helical milling parameters.

Funding information The paper is financially supported by the Natural Science Foundation of Shandong Province (ZR2015EL023), the National Natural Science Foundation of China (51505264), and the SDUT & Zibo City Integration Development Project (2017ZBXC189).

References

1. Pereira RBD, Leite RR, Alvim AC, Paiva APD, Ferreira JR, Davim JP (2017) Multi-objective robust optimization of the sustainable helical milling process of the aluminium alloy Al 7075 using the augmented-enhanced normalized normal constraint method. J Clean Prod 152:474–496
2. Qin XD, Lu C, Wang Q, Li H, Gui LJ (2012) Modal analysis of helical milling unit. Adv Mater Res 482–484:2454–2459
3. Wang H, Qin X, Ren C, Wang Q (2011) Prediction of cutting forces in helical milling process. Int J Adv Manuf Technol 58(9–12):849–859
4. Sakamoto S, Iwasa H (2012) Effect of cutting revolution speed on cutting temperature in helical milling of CFRP composite laminates. Key Eng Mater 523–524:58–63
5. Li H, He G, Qin X, Wang G, Lu C, Gui L (2014) Tool wear and hole quality investigation in dry helical milling of Ti-6Al-4V alloy. Int J Adv Manuf Technol 71(5–8):1511–1523
6. Qin X, Wang B, Wang G, Li H, Jiang Y, Zhang X (2014) Delamination analysis of the helical milling of carbon fiber-reinforced plastics by using the artificial neural network model. J Mech Sci Technol 28(2):713–719
7. Eguti CCA, Trabasso LG (2014) Design of a robotic orbital driller for assembling aircraft structures. Mechatronics 24(5):533–545
8. Li Z, Liu Q (2012) Surface topography and roughness in hole-making by helical milling. Int J Adv Manuf Technol 66(9–12): 1415–1425
9. Voss R, Henerichs M, Kuster F (2016) Corrigendum to "comparison of conventional drilling and orbital drilling in machining carbon fibre reinforced plastics (CFRP)". CIRP Ann Manuf Technol 65(1): 137–140
10. Dias D, Marques A (2015) Hole quality and cutting time evaluation in the interpolated helical milling. Int J Manuf Res 10(4):313–327
11. Pereira RBD, Brandao LC, Paiva APD, Ferreira JR, Davim JP (2017) A review of helical milling process. Int J Mach Tools Manuf 120:27–48
12. Cheng X, Wang ZG, Nakamoto K, Yamazaki K (2011) A study on the micro tooling for micro/nano milling. Int J Adv Manuf Technol 53(5):523–533
13. Bissaco G, Hansen HN, Chiffre LD (2005) Micromilling of hardened tool steel for mould making applications. J Mater Process Technol 167(2–3):201–207
14. Cheng X, Wei XT, Yang XH, Guo YB (2014) Unified criterion for brittle-ductile transition in mechanical microcutting of brittle materials. J Manuf Sci Eng 136(5):051013-1-7
15. Cheng X, Yang XH, Zheng GM, Huang YM, Li L (2014) Fabrication accuracy analysis of micromilling tools with complicated geometries by wire EDM. Mach Sci Technol 28(6):2329–2335
16. Oliveira FBD, Rodrigues AR, Coelho RT, Souza AFD (2015) Size effect and minimum chip thickness in micromilling. Int J Mach Tools Manuf 89:39–54